Impact of blue-green spatial characteristics on urban thermal comfort

Zifei Xu*, Meifang Hou and Yueshu Yu

Shanghai Institute of Technology, Shanghai, 201418, China

*daisy14xu@hotmail.com

Abstract. Currently, the process of urbanization is developing rapidly, but the neglect of urban environment and other factors has led to the emergence of some "urban diseases", such as urban heat island effect. It refers to the phenomenon that the temperature in the central area of a city is higher than that in the surrounding suburbs or countryside. The characteristics of urban heat island effect mainly include increasing energy consumption, worsening air quality, increasing health risks, and damaging ecological balance. Effective response measures are therefore essential to mitigate this phenomenon and its effects. The blue-green space in the city can alleviate the heat island effect and reduce the temperature of the surrounding environment, which is the so-called "cold island effect". Therefore, taking Hangzhou as an example, the study clarifies the pattern of urban blue-green space and then inversely calculates the pattern of cold island intensity in the study area. After clarifying the pattern of urban blue-green spaces, the study area is inverted to calculate the intensity pattern of cold islands, and indicators are screened to explore the influence factors of urban blue-green spaces on the intensity and spread of cold islands. The study shows that various blue-green spaces show an increasing trend of surface temperature as the distance from them increases, but then the changes will level off. And the diffusion range of cold island in 24 sampling points is between 100-1305.1 m, with an average of about 666.58 m. According to the classification of type and form, waters, green spaces and their combinations have different average diffusion ranges. In addition, these indicators are positively correlated, i.e., the higher the values of external watershed area and external impervious surface area, the higher the spreading range of cold islands. The study proposes targeted optimization strategies for urban blue-green spaces, which are of guidance and reference value for the construction and planning of urban blue-green spaces.

Keywords: Blue-green space, Cold island effect, Urban environment.

1 Introduction

In recent years, with the urban heat island effect intensifying year by year, high temperature and heat wave disasters also occur frequently, which has brought certain impacts on the public infrastructure of the city and the health of the residents, so the problem of mitigating the urban heat island effect is imminent[1]. Blue-green space

A. E. Abomohra et al. (eds.), *Proceedings of the 2023 9th International Conference on Advances in Energy Resources and Environment Engineering (ICAESEE 2023)*, Atlantis Highlights in Engineering 29,
https://doi.org/10.2991/978-94-6463-415-0_49

(BGS) is the spatial system composed of various kinds of open spaces such as waters, wetlands and green spaces in the national land space. BGS is not two separate systems, but a specific space of the life community of mountains, water, forests, fields, lakes and grasses[2-3]. As an important carrier to maintain the regional ecological environment, the dynamic characteristics of BGS are largely influenced by human activities. Under the background of rapid development of global urbanization, the problem of urban heat island is becoming more and more prominent, and BGS is an important way to mitigate the urban heat island, reduce energy consumption and improve air quality[4]. Currently, the research on BGS mainly focuses on the cold island (CI) effect, spatial and temporal distribution pattern, and driving factors of BGS [5]. Scholars such as Mabel L have explored in depth the role of such infrastructure in providing recreational, socio-ocultural and tourism value, in particular the economic assessment of such services. The findings highlight the important role of BGI in improving urban environmental quality and reveal its profound impact on urban quality of life and sustainability. Through this study, the value of BGI in urban planning can be more clearly defined, especially in highly dense urban environments like Singapore [6]. Relevant studies show that the inhibition effect of CI effect on heat island effect of BGS is significantly smaller than that of urban construction land, and the integration of BGS has a more significant effect on the inhibition of urban heat island[7]. In order to investigate the influence of the CI intensity pattern of urban BGS on urban thermal comfort, the study constructs the corresponding urban CI potential surface model through the screening of indicators and puts forward a scientific and reasonable urban BGS construction strategy according to the results of the study. The study aims to enhance the quality of urban habitat and improve the quality of life of the residents through rational planning of urban BGS, which in turn ensures the sustainable development of the society.

2 Subject of the study

2.1 Overview of the study area

Hangzhou, located along the southern edge of the Yangtze River Delta and the Qiantang River basin, belongs to the subtropical monsoon climate zone, with a year-round temperature of about 18°C, while the summer temperature rises year by year, and it has the title of the "New Four Hot Furnaces". The blue space status of Hangzhou is as follows: the city is blessed with hydrological conditions, with a dense network of rivers and the world's longest man-made canal, the Beijing-Hangzhou Grand Canal. In addition, Hangzhou's major rivers belong to the two water systems of Qiantang River and Taihu Lake. The density of the water network is 10km/km2 There are 470 rivers in the city, with a total length of nearly 1,000 km, of which 291 are more than 1km long, with a total length of about 900 km, and a water area of about 24 km2 The current status of green space in Hangzhou is as follows: the city is located in the subtropical monsoon climate zone, and is dominated by sub-tropical coniferous forests, deciduous broadleaf forests, and deciduous broadleaf forests. The forest coverage accounts for 62.8% of the city's total area and is rich in plant resources. The total area of forests is 16.89 million mu, with a total storage capacity of 67.9 million cubic meters. The Hangzhou Green-

land System Plan (Revision) (2007-2020) shows that the area of greenland in Hangzhou city is 1065.4km2, with a green coverage rate, greenland to urban construction land ratio, and park greenland service radius coverage rate of 40.58%, 24.05%, and 90%, respectively. The normalized vegetation area of the study area is 1598.3/km2 , which is 47.57% of the total area of the study area [8] .

2.2 Data sources and pre-processing

The study is based on the Landsat series of satellite images provided by the United States Geological Survey (USGS) to conduct land use type classification and surface temperature inversion research. The research shows that the strongest CI effect and heat island effect is in summer, so the study selects the Landsat satellite images in summer, which has the strongest contrast, as the object of the study. The downloaded remote sensing images need to be pre-processed appropriately, and the study firstly processed the existing satellite remote sensing images with band combination, geometric correction, atmospheric correction and image cropping[9] . The feature targets on the image can be made by band combining, while geometric correction can be used to correct the remote sensing images with serious deformation. Atmospheric correction refers to the absorption and scattering of the atmosphere and the interference of terrain during image acquisition[10] . Image clipping technique improves data processing efficiency and saves storage space by clipping the vector boundaries of the measured object and saving only the information of the measured object[11].

3 Research Methodology

3.1 Selection and Calculation of Factors Influencing the Urban CI Effect

The CI effect is mainly manifested in the degree of temperature reduction and diffusion area, so the study analyzes the influence mechanism of the CI effect from the CI intensity and CI diffusion. The CI intensity is the specific manifestation of the CI effect to reduce the temperature, which is affected by many factors. However, not every item can have an important impact on the urban thermal environment, so the relevant indicators should be initially screened first. In order to find out the index which is closely related to the cold island effect of urban blue and green space from the numerous alternative indicators, the following four principles should be followed. First, select indicators that can typically reflect the effect of blue-green space on the surrounding climate regulation. Secondly, the core index should change regularly with the change of the cold island effect. Furthermore, the options must be available and accurately quantified through field observations, remote sensing techniques, or other data acquisition methods. Finally, avoid repetition between different indicators. Urban function, ground cover, and urban buildings are taken as the three main indicators affecting the urban thermal environment. The subdivided indicators under the urban function indicator include population density (people/km^2) and GDP output value (10,000 yuan/km^2). The sub-indicators under the surface cover indicator include the proportion of

functional land (%), NDVI, the proportion of each surface cover (%), and DEM elevation (m). The sub-indicators under the urban building indicator include surface roughness (%), building density (%), and average number of building floors (%). Based on the previous study, it was found that the CI diffusion in BGS is affected by both internal and external factors. Therefore, the study divides it into internal elements of BGS and external elements of space, and establishes a CI diffusion index system as shown in Figure 1.

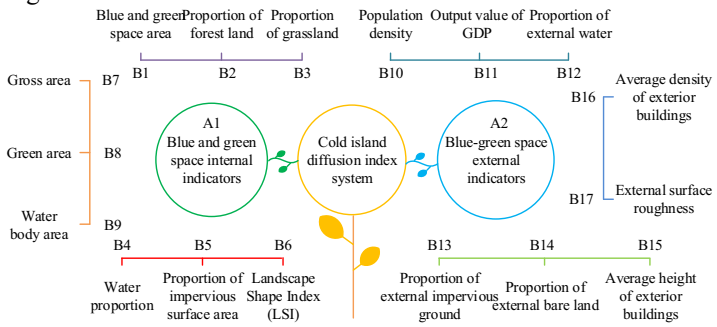

Fig. 1. CI diffusion indicator system

The "CI Intensity Index" and "CI Spatial Expansion Index" proposed in the study reflect the degree of influence of the CI effect in urban BGS. After screening, the CI intensity indexes are divided as follows: the internal indexes of BGS include the percentage of green space (%), the percentage of water body (%), the landscape shape index (LSI), the total area, the area of green space, and the area of water body. The internal indicators of BGS include external water body area, external impervious land area, building density (%), average number of building floors, and external surface roughness. Through the multiple regression analysis of CI intensity, the quantitative relationship between CI intensity and its core index is obtained, and then a more accurate correlation model is obtained[12]. The calculation process of this prediction model is shown in equation (1).

$$UCI = k_0 + k_1 RK + k_2 MD + k_3 AD + k_4 AD + k_5 RD + k_6 JM + k_7 LD + k_8 SY + k_9 BT + + k_{10} ND \quad (1)$$

In equation (1), RK denotes the population density. AD, BD, RD, MD The ratio of land use in Class A, B, R, and M, respectively, represents the average building density, and represents NDVI. JM represents the average building density, and ND represents NDVI. LD, SY, BT represents the proportion of water, green space, and impervious surface. In the meta-linear regression analysis, ND and RK were excluded because NDVI did not pass the covariance test and population density did not pass the significance test.

3.2 Surface temperature inversion and urban heat island effect quantification methods

Using Landsat series satellite images as a data source, several methods can be used to invert the surface temperature. Among them, the surface temperature inversion obtained by the radiative transfer equation method based on Landsat7ETM+ image data has higher accuracy, so the study utilizes this method to invert the surface temperature of the study area. First, the absolute radiant brightness received by the sensor is calculated by the radiative transfer equation, which is shown in equation (2).

$$L_l = G_a \bullet DN + O_f \tag{2}$$

In Eq. (2), Q denotes the gain and O_f is the offset. Secondly, the surface specific emissivity is estimated. The hybrid image element method was used in the study to calculate it and this computational expression is shown in equation (3).

$$\varepsilon = P_v R_v \varepsilon_v + \left(1 - P_v\right) R_S \varepsilon_S + d_\varepsilon \tag{3}$$

In Eq. (3), P_v represents the ratio of prepared cover, R_v represents the temperature ratio, and R_S is the temperature ratio of bare soil. $\varepsilon_v, \varepsilon_S$ Then, it represents the specific emissivity of vegetation and soil, respectively. d_ε The value of can be calculated according to equation (4).

$$P_v = \left(\frac{NDVI - NDVI_{MIN}}{NDVI_{MAX} - NDVI_{MIN}} \right)^2 \tag{4}$$

In Eq. (4), $NDVI$ denotes the index of normalized vegetation, and $NDVI_{MAX}, NDVI_{MIN}$ denotes the maximum and minimum values of the index in a certain area. And P_v is calculated according to equation (5).

$$d_\varepsilon = \begin{cases} 0.0038 P_v, P_v < 0.5 \\ 0.0038\left(1 - P_v\right), P_v > 0.5 \\ 0.0019, P_v = 0.5 \end{cases} \tag{5}$$

Since the urban surface mainly consists of different buildings and vegetation, the current specific emissivity studies for urban surfaces are mainly based on the hybrid image element method. The formula is shown in equation (6).

$$\varepsilon = P_v R_v \varepsilon_v + \left(1 - P_v\right) R_m \varepsilon_m + d\varepsilon \tag{6}$$

In equation (6), R_m represents the temperature ratio of the building surface. ε_m It represents the specific emissivity of the building surface. the values of Landsat8 band 10 for water bodies, vegetation, soil, and building surfaces ε are 0.995, 0.986, 0.972,

and 0.970 respectively . In the third step, the surface radiation values are calculated by equation (7).

$$\begin{cases} B(Ts) = \left[L_l - L_{a,i} \uparrow - \tau(1-\varepsilon) L_{a,i} \downarrow \right] / \tau\varepsilon \\ Ts = K_2 / \ln\left(K_1 / B(Ts) + 1\right) \end{cases} \tag{7}$$

In Eq. (7), Ts represents the surface temperature. $L_{a,i} \uparrow, L_{a,i} \downarrow$ represents the upward and downward radiant brightness of the atmosphere (W-m-2 -sr-1 -μm-1), respectively. τ represents the atmospheric transmittance in the red-hot outer band. K_1, K_2 Both represent the pre-set constants before launching, and the values of the two are somewhat different. The results of related studies show that the surface temperature based on airborne or satellite remote sensing thermal infrared image inversion is positively correlated with the air temperature and can be used as a measurable indicator for modeling the air temperature. Due to the differences in the surface temperature data obtained from Landsat satellite data, there are some limitations in directly using the surface temperature results based on the inverse performance of remote sensing images for comparison. Therefore, the study eliminates the data errors acquired from satellite data and improves the comparability of the inversion results by normalizing Landsat satellite data. The calculation process of surface temperature normalization processing is shown in equation (8).

$$T_i^{'} = \left(T_i - T_{\min}\right) / \left(T_{\max} - T_{\min}\right) \tag{8}$$

In Eq. (8), T_i represents the surface temperature corresponding to the i th pixel. $T_{\max}, T_{\min}$ represent the highest and lowest surface temperatures in the study area, respectively. The heat island effect of the city is classified according to a gradient of 0.2 by normalization, and the value intervals of strong heat island, heat island, normal temperature, CI, and strong CI correspond to [0.8, 1], [0.6, 0.8], [0.4, 0.6], [0.2, 0.4], and [0, 0.2], respectively. In addition, using local spatial autocorrelation analysis methods, hot and cold clusters in the city can be distinguished. Therefore, an image analysis method called "beyond pixel" is used to obtain relatively homogeneous surface temperature data with continuous geographic boundaries.

4 Analysis of urban BGS characteristics' impact on thermal comfort

In order to explore the quantitative relationship between CI intensity and each indicator, the study utilized ArcGis software to perform grid division and sampling with 500×500 m as the boundary. At the same time, the surface temperature and the spatial distribution elements of urban functions, buildings, and surface cover indicators were superimposed, and then the relationship between the intensity of CI and each indicator was explored in the BGS. In order to study the relationship between the intensity of CI and the indicators of urban function, urban buildings and urban surface cover, the data

of the indicators of urban function and the CI intensity in the sampling points were linearly fitted using SPSS.23, and the results are shown in Table 1.

Table 1. Results of linear fitting of CI intensity to each indicator

Index	Equation	R2	Adjusted R2
GDP	y=1.2442+-2.57195E-5*x	0.07354	0.07329
population	y=1.47247+-2.08303E-4*x	0.13889	0.13867
RD	y=-0.49119+-0.00496*x	0.00551	0.00477
BD	y=-0.9989+-0.00733*x	0.0065	0.00512
AD	y=-0.74301+-0.005*x	0.00489	0.00382
MD	y=-0.33518+-0.03356*x	0.27667	0.27603
Average building density	y=-0.12584+-5.65642*x	0.15627	0.15568
Average number of building floors	y=-1.00353+-0.03277*x	0.00558	0.00488
Surface roughness	y=-0.90852+-0.00743*x	4.8246E-4	-2.1504E-4
SY	y=-1.92679+-0.04952*x	0.56455	0.56443
LD	y=0.66335+-0.0477*x	0.19628	0.19597
BT	y=2.85548+-0.05341*x	0.69852	0.69843
The proportion of bare land	y=-1.53455+-0.12237*x	0.17961	0.17846
DEM	y=0.19224+-0.0165*x	0.01056	0.0103
ND	y=-1.93003+-13.2364*x	0.21658	0.21638

As can be seen from Table 1, population and M-type land share exhibit a positive univariate linear relationship with the intensity of the CI effect, and both pass the 5% significance test, indicating that they have very good explanatory power for the intensity of the CI effect. In addition, urban building characteristics, particularly average building density, were also found to have a valid linear fit with the intensity of the CI. An increase in building density seems to lead to an enhancement of the CI effect, and this relationship again passes the 5% significance level. Whereas an increase in the number of building floors and ground roughness had a positive relationship with the enhancement of CIs, the CI effect was more pronounced in these areas with higher heights and roughness. Surface cover factors such as the proportion of green space, water, and impervious surfaces, along with NDVI, also showed significant linear correlations with CI intensity. When the proportion of green space or water was increased, the intensity of the CI became larger. In contrast, an increase in the proportion of impervious surfaces and bare soil surfaces is associated with a weakening of the CI effect. By monitoring and managing these key indicators, the urban CI effect can be more effectively controlled and mitigated, thus improving the ecological environment of the city and the quality of life of the residents. The main data source of the experiment is Landsat8 satellite data with 30-meter spatial resolution. In order to ensure the accuracy of the study and to consider possible errors, urban BGS with an area of more than 1 hectare was selected as the study object. A total of 24 BGSs within the selected study area were chosen as sample points for analysis. Figure 2 shows the extent of CI diffusion in each BGS.

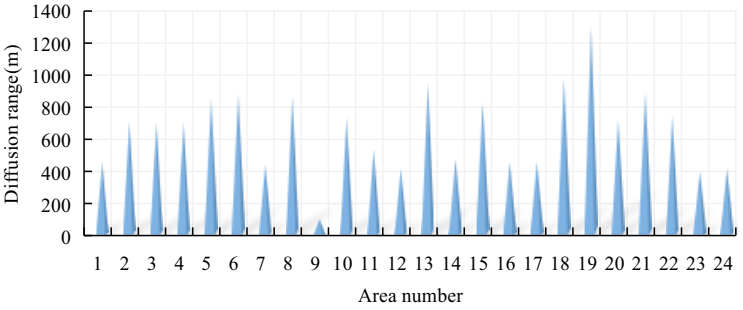

Fig. 2. Extent of CI diffusion in each BGS

As can be seen from Figure 2, each BGS shows the trend of temperature increase with distance away from the BGS, but when the distance reaches a certain value, the change of surface temperature with the increase of distance tends to level off. That is, the CI effect of the BGS has a certain range of influence, that is, the range of CI diffusion. In your study area, the range of CI diffusion is between 100-1305.1 m, and the average diffusion range is about 666.58 m. Further, this range seems to be affected by different types and forms of BGS. The average diffusion range for water only is 675.6m, while the average diffusion range for green space only is 641m. furthermore, based on the morphology, the average diffusion range for banded is 673.9m, and the average diffusion range for faceted is 677.6m. the results of the fit of CI diffusion to the internal metrics of the BGS are shown in Figure 3.

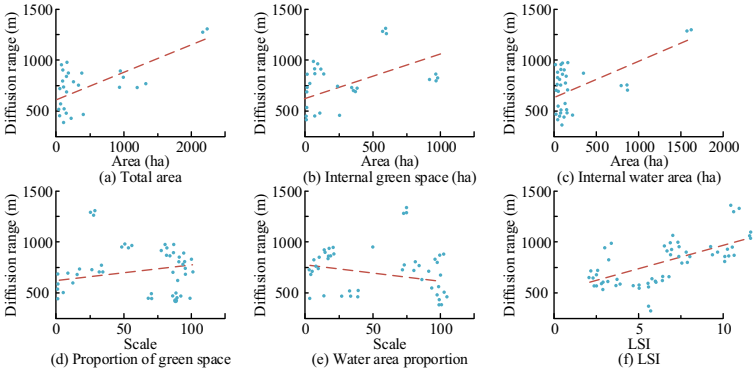

Fig. 3. Fitted relationship between CI diffusion and indicators within the BGS

As can be seen from Fig. 3, the blue-green spatial interior indicators have a good role in explaining the changes in the spreading range of CIs, especially the LSI indicators show a good univariate linear fitting relationship with the spreading range of CIs, and the fitting results all pass the 0.05 significance level test. This indicates that the growth of LSI plays a positive role on the spreading range of CI. Meanwhile, the total area, green space area, water area and its share also seem to be closely related to the CI diffusion range. The results of fitting the CI spread with the external indicators of blue and green space are shown in Figure 4.

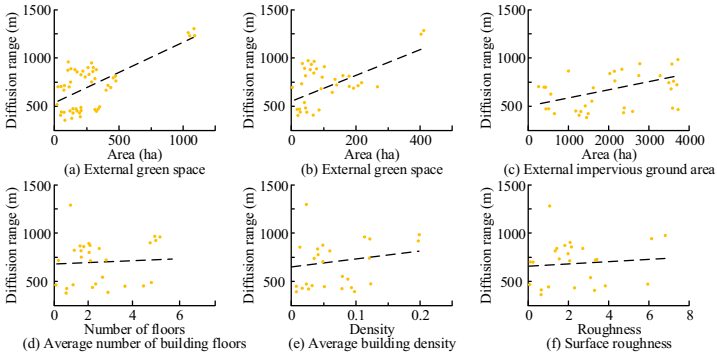

Fig. 4. Fitted relationship between CI diffusion and external indicators of BGS

As can be seen from Figure 4, there is a good one-dimensional linear fitting relationship between external green space area, external water area and external impervious surface area, which plays a key role in explaining the changes in the spreading range of CIs. In particular, the effect of external green space area on the spreading extent of CIs is particularly significant, and the fitting results all pass the 0.05 significance level test. In addition, among these indicators, the influence on the spreading range of CI is the largest, and the larger its area is, the wider the spreading range of CI is. Moreover, the indicators are positively correlated, i.e., the higher the values of external water area and external impervious surface area, the higher the spreading range of CIs.

5 Conclusion

The study used techniques such as remote sensing and GIS, combined with landscape ecology, urban planning and statistics, to carry out a fundamental study of the CI effect and cooling effectiveness for the main urban area of Hangzhou. The study shows that various BGSs show an increasing trend in surface temperature as the distance from them increases, but then the change will level off. And the diffusion range of CIs in 24 sampling points is between 100-1305.1 m, with an average of about 666.58 m. According to the classification of types and forms, waters, green spaces and their combinations have different average diffusion ranges. In addition, among these indicators, the larger its area, the wider the range of CI diffusion. Moreover, the indicators are positively correlated, i.e., the higher the values of external watershed area and external impervious surface area, the higher the spreading range of CIs. For this reason, the study proposes to increase the area of green and blue space in the weak potential zone and suggests the use of green seams and the construction of green roofs. The construction of hot and cold corridors to connect weak and strong potential areas; for the agglomeration area should take a higher priority for remediation, which can be combined with the construction of urban ventilation corridors and urban ecological networks for remediation and construction.

References

1. Fisher, J, C., Bicknell, J, E., Irvine, K, N., Hayes, W, M., Davies, Z, G.: Bird diversity and psychological well-being: a comparison of green and coastal blue space in a neotropical city. Science of The Total Environment 793(1), 1-8 (2021).
2. Plummer, I., Liu, Y., Sieving, K, E.: Urban Greenspace is for the Bluebirds: Nest-Box Selection across a Noise Gradient on an Urbanizing University Campus. Southeastern Naturalist 20(1), 152-161 (2021).
3. Sivaranjani, A., Senthilrani, S.: Computer Vision-Based Cashew Nuts Grading System Using Machine Learning Methods. and Computers 32(3), 1-22 (2023).
4. Chorol, L., Gupta, S, K.: Evaluation of groundwater heavy metal pollution index through analytical hierarchy process and its health risk assessment via Monte Carlo simulation. process Safety and Environmental Protection 170, 855-864 (2023).
5. Yang, H., Dong, C., Zhang, H., Luo, H., Li, J., Yin, J.: Characteristics and Source Analysis of Soil Heavy Metal Pollution in a Mining Area. Journal of Earth Sciences Journal of Earth Sciences and Environmental Protection 10(3), 159-176 (2022).
6. Mabel, L., Stefanos, X.: Economic assessment of urban space and blue-green infrastructure in Singapore. Journal of Urban Ecology 7(1), 1-11(2021).
7. Sheeja, K, M., Harilal, C, C.: Spatial distribution and seasonal variation of heavy metal contaminants and pollution indices in a coastal landmass of Kerala, peninsular India. Chemistry and Ecology 38(1/5), 211-232 (2022).
8. Chen, P., Wu, Y., Wang, Y.: Optical fibre Fabry-Perot temperature sensor based on metal welding technology. Journal of Nanophotonics 17(1), 1-8 (2023).
9. Choudhuri, S., Adeniye, S. Sen, A.: Distribution Alignment Using Complement Entropy Objective and Adaptive Consensus-Based Label Refinement For Partial Domain Adaptation," AIA 1(1), 43-51 (2023).
10. Lin, S., Zhang, Y., Qu, Y., Han, X.: A Miniature high-temperature fiber-optic sensor based on tip-packaged Fabry-Perot interferometer. Sensors and Actuators A: Physical 350, 1-5 (2023).
11. Ahn, Y., Yun, H, S., Pandi, Kl.: Heavy metal speciation with prediction model for heavy metal mobility and risk assessment in mine-affected soils. Environmental Science and Pollution Research 27(3), 3213-3223 (2020).
12. Zhong, Y., Yang, J., Wang, S.: Sensor-based characteristics of kaolin and the adsorption of heavy metal ions. Arabian Journal of Geosciences 14(16), 2-16 (2020).